10th Canadian Masonry Symposium, Banff, Alberta, June 8 – 12, 2005

NUMERICAL SIMULATION OF URM WALLS RETROFITTED WITH CABLE BY DISTINCT ELEMENT METHOD

Y. Zhuge[1]

[1]Senior Lecturer, School of Natural and Built Environments, University of South Australia, Mawson Lakes Campus, SA 5095, Australia, yan.zhuge@unisa.edu.au

ABSTRACT

The history of past earthquakes has shown that masonry buildings have suffered the maximum damage. Also, the Australian love of "heritage" buildings (most of them being of unreinforced masonry) means that greater attention is required to secure their performance under seismic loading in the future. Therefore, to retrofit and strengthen existing masonry structures to resist potential damage from earthquakes has become an important issue.

A research project was carried out at the University of South Australia aimed at developing a simple and high strength seismic retrofitting technique for masonry structures. A series of experimental tests on unreinforced masonry (URM) walls retrofitted with an innovative cable system have been conducted. The results indicated that both the strength and ductility of the tested specimens were significantly enhanced with the technique.

In this paper, an analytical model based on Distinct Element Method (DEM) has been developed to simulate the behaviour of URM walls before and after retrofitting.

KEYWORDS: distinct element method, walls, retrofitting, cable.

INTRODUCTION

The Newcastle earthquake in 1989 led to the creation of a new set of guidelines for earthquake resistant design in Australia. This new code has resulted in the need to retrofit structures that do not comply with the new guidelines systematically. Masonry structures are one of the most common construction types in Australia. Although the history of past earthquakes has shown that masonry buildings have suffered the maximum damage and also accounted for the maximum loss of life, they continue to be popular. Most of the historical buildings throughout Australia are unreinforced masonry (URM), highlighting the need to improve their performance by retrofitting and strengthening to resist potential earthquake damage.

Two types of failure are commonly observed in load bearing URM walls subjected to seismic loads. These are in-plane failure characterized by a diagonal tensile crack pattern, and out-of-plane failure, where cracks are primarily along the mortar bed joints. The current research project is aimed at increasing the in-plane load carrying capacity of URM walls. A series of experimental tests on URM walls retrofitted with an innovative cable system have been conducted. The results indicated that both the strength and ductility of tested specimens were significantly enhanced with the technique.

In this paper, an analytical model which is based on Distinct Element Method (DEM) has been developed to simulate the behaviour of URM walls before and after retrofitting. In the distinct element method, a solid is represented as an assembly of discrete blocks. Joints are modelled as interfaces between distinct bodies. The DEM is a dynamic process especially designed to model the behaviour of discontinuities. By using DEM, the response of discontinuous media, such as unreinforced masonry, under both static and dynamic loading can be simulated.

The DEM model was successfully applied to simulate the response of URM shear wall panels in previous studies [1, 2]. In the current study, a new user defined FISH function has been developed to model the structural behaviour of cable. The results between distinct element model and experiments are compared and discussed.

OUTLINE OF DISTINCT ELEMENT METHOD

The Distinct Element Method has been progressively developed over the past two decades. Cundall [3] first introduced the Distinct Element Method to simulate progressive movements in block-like rock systems and the model has been implemented subsequently into the computer program UDEC.

In the DEM method, a solid is represented as an assembly of discrete blocks. Joints are modelled as interfaces between distinct bodies. The contact forces and displacements at the interfaces of a stressed assembly of blocks are found through a series of calculations, which trace the movements of the blocks [4]. At all the contacts, either rigid or deformable blocks are connected by spring-like joints with normal and shear stiffness k_n and k_s respectively. Similar to the Finite Element Method (FEM), the unknowns in the DEM are also the nodal displacements and rotations of the blocks. However, unlike FEM, DEM is a dynamic process and the unknowns are solved by the equations of motion. The speed of propagation depends on the physical properties of the discrete system. The solution scheme used by DEM is the explicit time marching scheme and it uses finite contact stiffness.

If the blocks are rigid, block displacements are calculated from the out of balance moment and forces applied to the centre of gravity of each block. Resultant forces F include boundary forces applied to the edges of the block and gravity.

Newton's second law of motion is applied for each block:

$$\frac{\partial \dot{u}^{(t)}}{\partial t} = \frac{F^{(t)}}{m} \qquad \text{Equation 1}$$

where $\dot{u}$ is the velocity, m is the mass, and t is the time.

Following the central difference integration scheme, Equation 1 can be transformed into:

$$\dot{u}^{(t+\Delta t/2)} = \dot{u}^{(t-\Delta t/2)} + \frac{F^{(t)}}{m}\Delta t \qquad \text{Equation 2}$$

For blocks in two dimensions where several forces are assumed to act on the block (including gravity loads), the velocity (Equation 2) can be re-arranged to include the angular velocity of block:

$$\dot{u}_i^{(t+\Delta t/2)} = \dot{u}_i^{(t-\Delta t/2)} + \left(\frac{\sum F_i^{(t)}}{m} + g_i\right)\Delta t$$

$$\dot{q}^{(t+\Delta t/2)} = \dot{q}^{(t-\Delta t/2)} + \left(\frac{\sum M^{(t)}}{I}\right)\Delta t \qquad \text{Equation 3}$$

where $\dot{q}$ = the angular velocity of the block; I = the moment of inertia of the block; $\dot{u}_i$ = the velocity components of block centroid; $\Sigma M^{(t)}$ = the total moment acting on the block; $\Sigma F_i^{(t)}$ = the total force acting on the block; and g_i = the components of gravitational acceleration.

Assuming the velocities are stored at the half-time point of the step, the new velocities in Equation 3 can be used to determine the new block location:

$$x_i^{(t+\Delta t)} = x_i^{(t)} + \dot{u}_i^{(t+\Delta t/2)}\Delta t$$

$$q^{(t+\Delta t)} = q^{(t)} + \dot{q}^{(t+\Delta t/2}\Delta t \qquad \text{Equation 4}$$

where θ = the rotation of the block about its centroid; and x_i = the coordinates of block centroid.

The new position of the block induces new conditions at the block boundaries and thus new contact forces. Resultant forces and moments are used to calculate the linear and angular accelerations of each block. The calculation scheme summarised above by Equation 1 to Equation 4 is repeated until a satisfactory state of equilibrium or continuing failure is reached for each block. It should be noted that time has no real physical meaning if a static analysis is being performed.

If the blocks are deformable, they will first be internally discretised into finite difference triangular elements before the equations of motion are formulated at each grid point.

The mortar joints are represented numerically as a contact surface between two block edges. The constitutive laws applied to the contacts are:

$$\Delta s_n = k_n \Delta u_n \qquad \text{Equation 5}$$

$$\Delta t_s = k_s \Delta u_s \qquad \text{Equation 6}$$

where k_n and k_s are the normal and shear stiffness of the contact, $\Delta\sigma_n$ and $\Delta\tau_s$ are the effective normal and shear stress increments, and Δu_n and Δu_s are the normal and shear displacement increments.

Stresses calculated at grid points located along contacts are submitted to the selected failure criterion. For unreinforced masonry shear wall panels, Coulomb friction is formulated:

$$\left|\tau_s\right| \leq C + \sigma_n \tan\phi = \tau_{\max} \qquad \text{Equation 7}$$

where C is the cohesion and ϕ is the friction angle.

There is also a limiting tensile strength f_t for the joint. If the tensile strength is exceeded, then $\sigma_n = 0$.

Modelling direct tensile splitting of brick is a more delicate subject. In order to simplify the problem, the brick unit material is modelled with a Mohr-Coulomb failure criterion with a tension cutoff. The shear flow rule is non-associated and the tensile flow rule is associated.

A detailed discussion of the model can be found in Zhuge and Hunt [3].

SUMMARY OF EXPERIMENTAL PROCEDURES

Three full-scale clay brick masonry walls retrofitted with the cable system have been tested under combined compression and racking cyclic loads. An unreinforced masonry wall was also tested under the same loading condition for comparison.

The proposed retrofitting systems aim to improve the performance of walls by increasing shear strength above flexural strength and by increasing ductility and energy dissipation capability. All specimens were chosen with an aspect ratio of 1.0 to ensure that most of the unretrofitted walls would exhibit shear-induced damage. Therefore, in-plane failure would dominate. The dimensions of the wall were 940 mm long x 940 mm high x 110 mm wide (11 courses high and 4 bricks in each course). The wall was constructed on a concrete foundation beam to simulate a house footing.

The type of cable used for the experiment was Ronstan typical grade 316 stainless steel wire rope (19 single strands, diameter 10mm, breaking load 71 kN). The endings for the cable were seafast threaded swage terminals (RF1513M1010). The anchorage for the connection plate to the foundation beam was a Ramset Chemset Anchor (M 16 x 190 mm, design tensile and shear load 8.5 kN per anchor and Chemset 800 series). The cables were fixed on one side of the wall only.

Retrofit was accomplished by adding two 10 mm diameter cables (wire ropes) to one side of the wall face, as shown in Figure 1. Ideally cables should be added on both sides of the wall to prevent an eccentric stiffness and strength distribution that may cause twisting of the retrofitted walls. The cable diameter was chosen to ensure that the wall would fail earlier than the cable. The anchor was designed to transfer the load from the cable to the foundation without failure before the cable was broken.

The tested walls were subjected to a constant vertical compressive stress σ_m = 0.2 MPa. To simulate earthquake loading, a series of horizontal displacement reversals of increasing amplitude were applied to the walls. Each wall was cycled twice at each of the incrementally increasing displacement amplitudes until failure. The specimens were instrumented for displacement, rotation and strain measurements. Strain gauges were used to measure strains in cable.

Figure 1 – URM Wall Retrofitted with Cable [5]

NUMERICAL SIMULATION OF MASONRY WALLS RETROFITTED WITH CABLE

The cable consists of a number of wires or strands and has high tensile strength, lightness and high corrosion resistance. These materials can absorb tensile stress and increase overall element stiffness, ductility and bearing capacity. Using a cable system for seismic retrofitting applications has other advantages such as architectural versatility, low cost and fast construction, durability, and no loss of valuable space. Furthermore, it does not add a significant mass to the existing building, leaving the dynamic properties of the structures virtually unchanged.

Numerical simulation of URM walls retrofitted with a cable is not an easy task. First, masonry is not a simple material, as it is composed of two materials in a geometric array - an assemblage of bricks set in a mortar matrix. The influence of mortar joints and bond as a plane of weakness is a significant feature. A complicated two-phase finite element micro-model has been used by some researchers in recent years [6, 7, 8] but such a model would make this analysis very complex.

On the other hand, DEM is fully dynamic and deals with pseudo-static problems by allowing the dynamic behaviour to reach equilibrium with notional time. It is specially designed to model the behaviour of discontinuities. Therefore, DEM is well suited for masonry structures. The DEM has been applied by the author to analyse the structural behaviour of unreinforced masonry [3, 9]. Initially, a stress boundary was used, where the horizontal load was monotonically increased. However, neither the failure pattern nor the principal stress distribution compared well with experimental or finite element results. An improved model was then introduced, where the stress boundary was replaced by a progressively increased displacement boundary. The model was applied to simulate the response of unreinforced masonry shear wall panels with and without an opening, where experimental test results are available. In general, good agreement was observed in the comparison [3].

Although DEM has been successfully applied to simulate URM walls subject to in-plane load, adding a cable is not straightforward. A special cable element was created in the model to simulate the axial behaviour of the cable reinforcement which only carries uniaxial tensile force.

The incremental axial force, ΔF^t, is calculated from the incremental axial displacement by

$$\Delta F^t = -\frac{EA}{L}\Delta u^t \qquad \text{Equation 8}$$

where $\Delta u^t = \Delta u_i t_i = \Delta u_1 t_1 + \Delta u_2 t_2$. Subscript 1 and 2 correspond to the x-direction and the y-direction respectively.

The cable is assumed to be divided into a number of segments to pass through the joints that are required to be reinforced, with nodal points located at each segment end. Axial displacements are computed based on integration of the laws of motion using the computed out-of-balance axial force and a mass lumped at each nodal point (Itasca 2000). Different material properties were assigned to the unbonded section and the anchorage sections at the ends of the cable. In order to simulate the anchor connection to the end of the cable, a high grout shear stiffness and shear strength are assigned to the cable nodes embedded in the small blocks to which the cable is anchored. The material properties of the cable are listed in Table 1.

Table 1 – Material Properties of the Cable

	Cable		Unbonded section		Anchorage section	
E (MPa)	A (mm^2)	f_t (kN)	kbond (MPa)	sbond (MN/m)	kbond (MPa)	sbond (MN/m)
107500	78.5	71	1e-3	0	100	100

Where kbond is the grout shear stiffness and sbond is the cohesive strength of the grout.

k_n and k_s of the interfaces between the wall blocks are potentially important parameters in the numerical analyses of masonry walls using DEM . Unfortunately, there are very few test data available on stiffness properties of mortar joints. The only test results the authors could find were the experiments conducted at the University of Delft, the Netherlands [7]. These test results were used to validate the numerical model of masonry shear wall panels under in-plane lateral load developed by the authors [3]. As the parametric studies indicated that the sensitivity of the results with respect to the estimation of joint material parameters was small, these values of k_n and k_s have been adopted again for the current model (Table 2).

Table 2 - Summary of joint material properties

Tension	**Shear**			**Normal stiffness**	**Shear stiffness**
f_t (N/mm^2)	$\tan\phi$	$\tan\psi$	C (MPa)	k_n (N/mm^3)	k_s (N/mm^3)
0.25	0.75	0.0	0.375	82	36

Numerical modelling of each URM wall and URM wall retrofitted with cables was carried out using the distinct element code UDEC (Universal Distinct Element Code) [4]. The dimensions of the wall were based on the experimental program (Figure 1). Deformable blocks were utilised to enable force transmission between the wall and the cable. The deformable blocks must be discretised into finite difference triangular elements. The DEM model and a typical discrete element mesh are shown in Figure 2.

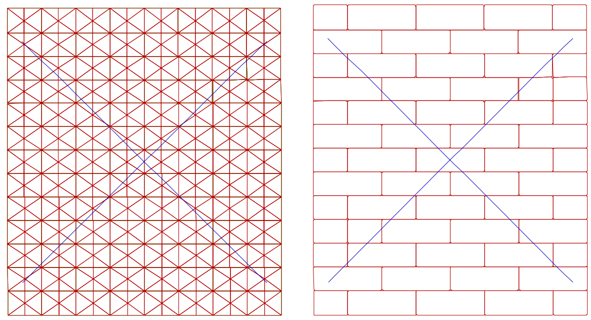

Figure 2 - URM Wall Retrofitted with Cable using UDEC

COMPARISON WITH EXPERIMENTAL INVESTIGATIONS

The comparison between numerical and experimental load-displacement diagrams is shown in Figure 3. It can be seen from the figure that the experimental behaviour is well simulated by the numerical model. The collapse load estimated by the numerical model was 40.7 kN compared to the experimental result of 39.1 kN (wall 2 in the diagram), and the average collapse load of all tested walls was 43.4 kN. The sudden load drop of around 20 kN was due to major diagonal cracking occurring in the wall. The diagram also indicates that the wall behaved in a quite ductile manner, which agrees with the experimental observations.

The force carried by the cable and the force carried by the retrofitted wall are also compared in Figure 3. The experimental results indicated that the cable carried around 50% of the force acting on the whole wall. However, the numerical results predicted that the cable would carry around 80% of the force when the wall reached its ultimate strength. Due to the limitation of the software and DEM, it is very difficult to model a steel plate attached to URM walls. Therefore, equivalent bond stiffness and strength were assigned to the cable wall connection. Nevertheless, the ultimate load capacity of the wall is well predicted by the model.

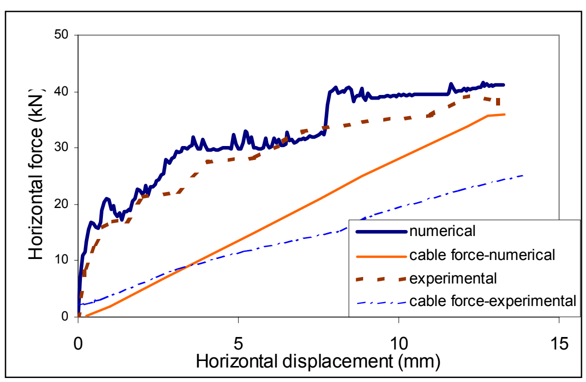

Figure 3 – Comparison of Load-deflection Behaviour

During the testing, all retrofitted walls exhibited superior behaviour when compared with URM walls. The ultimate load capacity of walls retrofitted with the cable was increased by around a factor of 2. As indicated by Figure 4, similar results are predicted by the numerical model. When a wall is retrofitted with a cable, the appearance of the crack cannot be prevented (similar cracking loads were predicted for walls with and without cables, indicated by a sudden drop in load around 20 kN). However, the behaviour of the walls would be quite different after the formation of the diagonal cracks. For the URM wall, major cracks developed along the diagonal direction, the wall failed due to compressive crushing at the supports and rotated as a rigid body. For the wall retrofitted with the cable, the cable could prevent the development of the main diagonal cracks, allowing the cracks to spread more evenly over the entire wall. The wall then could continue to carry higher load. This also agrees with the experimental results.

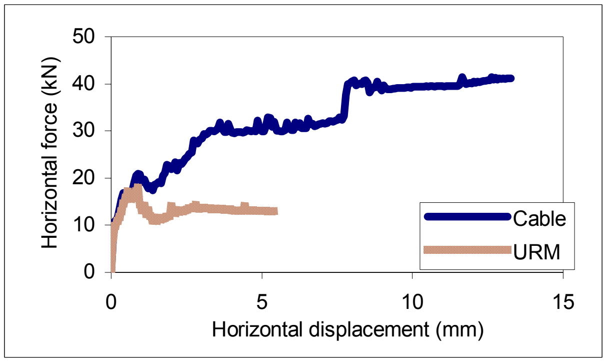

Figure 4 - Simulated Behaviour of the Wall with and without Cable – DEM Model

The above discussion of wall behaviour can be demonstrated by the minimum principal stresses distribution shown in Figure 5. For the URM wall (Figure 5(a)), when the diagonal cracks are fully open, two distinct struts are formed, one at each side of the diagonal crack. The concentration of the large compressive stress at the supports leads to the collapse of the wall. However, for the retrofitted wall (Figure 5(b)), the full opening of the diagonal cracks was prevented by the existence of the cable. Two distinct struts are not formed. A more continuous stress distribution is observed.

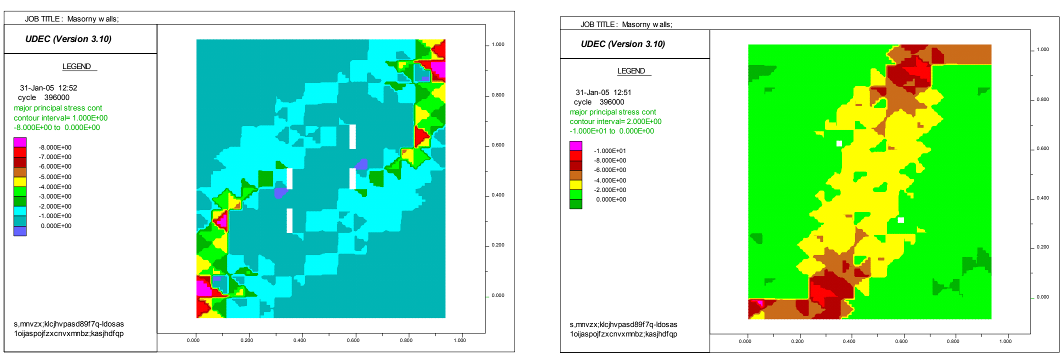

(a) URM wall **(b) Retrofitted wall**

Figure 5 - Principal Stress Distributions from DEM at a Displacement of 2.7 mm

The tensile and shear cracks that develop at the same displacement of 2.7 mm for walls with and without a cable predicted by the numerical model are illustrated in Figure 6. For the URM wall (Figure 6(a)), two stepped diagonal cracks through the head and bed joints are formed at this loading stage. For a wall retrofitted with a cable under the same displacement, only horizontal tensile cracks are developed along the top and bottom of the wall; no major diagonal cracks are formed (Figure 6(b)). This proved further that the load transmission path and the cracking patterns of the wall are changed when cable retrofitting is introduced.

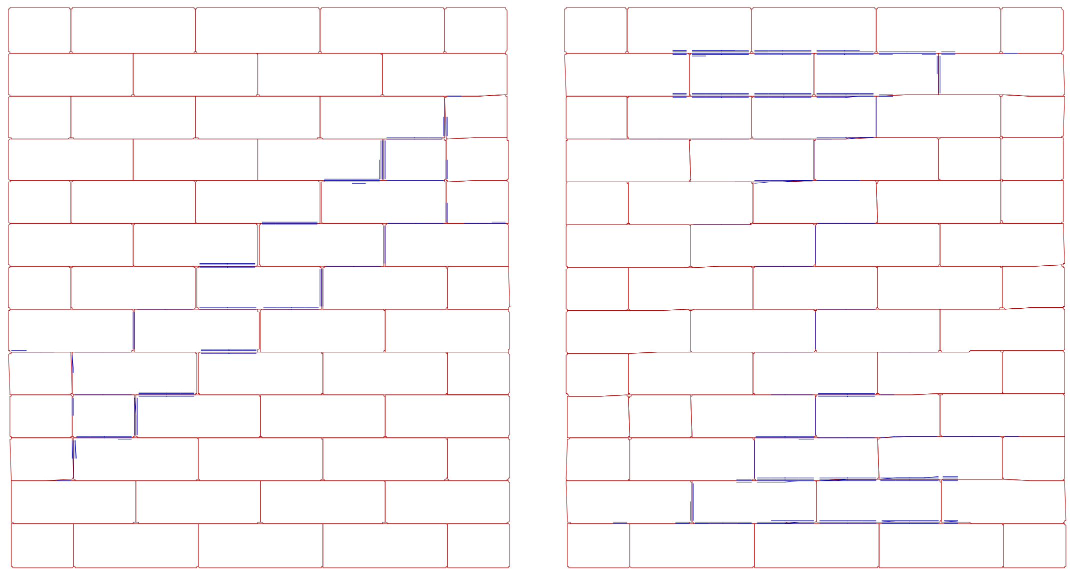

(a) URM wall **(b) Wall retrofitted with cable**

Figure 6 - Crack Patterns of the Analysis using DEM at a Displacement of 2.7 mm

CONCLUSIONS

Numerical modelling of masonry is not an easy task due the influence of mortar joints as planes of weakness. In the past few years, an alternative and simple way of modelling masonry using the Distinct Element Method has been developed and validated by experimental results. In this paper, the model is further developed to simulate the behaviour of unreinforced masonry walls before and after retrofitting with a cable system.

The model is validated by comparing the results with those obtained from experiments, which include the force-displacement diagram, ultimate load capacity and the failure pattern of the wall with and without retrofitting. The analysis has confirmed the experimental results that using a simple cable system to retrofit low-rise masonry walls is an effective technique to increase significantly the in-plane strength, ductility, and energy dissipation capacity. The improvement in the ultimate lateral load resistance of the retrofitted walls with cables is around two times the capacity of URM wall.

REFERENCES

1. Zhuge, Y. and Hunt, S. An Improved Distinct Element Model for Masonry Shear Panels. Proceedings of the Second International Conference on Advances in Structural Engineering and Mechanics, Busan, Korea, 2002.
2. Zhuge, Y. and Hunt, S. Numerical Simulation of Masonry Shear Panels with Distinct Element Approach. Structural Eng. And Mechanics – an International Journal, Vol. 15, No4, 2003, pp. 477–493.
3. Cundall, P. A. A Computer Model for Simulating Progressive Large Scale Movements in Blocky Rock Systems. Proceedings of the Sym. of the International Society for Rock mechanics, Nancy, Francs, Vol. 1, II-8, 1971, pp. 11-18.
4. ITASCA Consulting Group. Universal Distinct Element Code. ITASCA consulting Group, Inc., Minneapolis, Minnesota, USA, 2000.

5. Chuang, S, Zhuge, Y. and McBean, P. Experimental Testing of Unreinforced Masonry Walls Retrofitted by Cable System. Proceedings of the 7th Australasian Masonry Conference, Newcastle, 2004, pp 527-536.
6. Lotfi, H. and Shing, P. Interface Model Applied to Fracture of Masonry Structure. Journal of Structural Eng. ASCE, 1994, pp. 63-80.
7. Lourenco, P. B. Computational Strategies for Masonry Structures. PhD Thesis, Delft University of Technology, The Netherlands, 1996.
8. Gambarotta, L. and Lagomarsino, S. Damage Models for the Seismic Response of Brick Masonry Shear Walls. Part II: the continuum model and its applications. Earthquake Engineering & Structural Dynamics, 26, 1997, pp. 441-462.
9. Zhuge, Y. Distinct Element Modelling of Unreinforced Masonry Walls. Proc. of the 7th East Asia-Pacific Conference of Structural Eng. and Construction, Kochi, Japan, 1999, pp. 411-416.